Climate pathways behind phytoplankton-induced atmospheric warming

Rémy Asselot [1], Frank Lunkeit [2], Philip Holden [3], and Inga Hense [1]

[1]Institute for Marine Ecosystem and Fishery Science, Center for Earth System Research and Sustainability, University of Hamburg, Hamburg, Germany
[2]Meteorological Institute, Center for Earth System Research and Sustainability, University of Hamburg, Hamburg, Germany
[3]Environment, Earth and Ecosystems, The Open University, Walton Hall, Milton Keynes, MK7 6AA, UK

Correspondence: Rémy Asselot (remy.asselot@uni-hamburg.de)

Abstract. We investigate in which ways marine biologically-mediated heating increases the surface atmospheric temperature. While the effects of phytoplankton light absorption on the ocean have gained attention over the past years, the impact of this biogeophysical mechanism on the atmosphere is still unclear. Phytoplankton light absorption warms the surface of the ocean ~~with consequences for~~ which in turn affects the air-sea heat ~~exchange~~ and CO_2 ~~flux. We focus on the ocean-atmosphere interface and study the importance~~ exchanges. However, the contribution of air-sea heat ~~exchange versus air-sea~~ versus CO_2 ~~flux. To shed light on the role of phytoplankton light absorption on the surface atmospheric temperature, we performed different simulations with the EcoGENIE Earth system model. We configure the model without a seasonal cycle and, if not stated otherwise, the atmospheric CO_2 concentration is allowed to evolve freely. The climate pathways examined are :~~ fluxes in the phytoplankton-induced atmospheric warming has not been yet determined. Different so-called climate pathways are involved. We distinguish heat exchange, CO_2 exchange, dissolved CO_2, solubility of CO_2 ~~,~~ and sea-ice covered area. ~~Overall we show that the~~ To shed light, we employ the EcoGEnIE Earth system model that includes a new light penetration scheme and isolate the effects of individual fluxes. Our results indicate that phytoplankton-induced changes in air-sea CO_2 exchange ~~has a larger effect on the biologically-induced atmospheric warming than the~~ warm the atmosphere by 0.71°C due to higher greenhouse gas concentrations. The phytoplankton-induced changes in air-sea heat ~~flux. Moreover, we notice that the freely evolving solubility of~~ exchange cool the atmosphere by 0.02°C due to a larger outgoing longwave radiation. Overall, the enhanced air-sea CO_2 ~~has a cooling effect on the surface atmospheric temperature~~exchange due to phytoplankton light absorption is the main driver in the biologically-induced atmospheric heating.

1 Introduction

Previous studies have shown that marine biota can modify the light penetration in the ocean with consequences on the atmospheric temperature and on the climate system (**???**). Using an Earth system model (ESM) of intermediate complexity, we

identify and compare the climate pathways behind the changes in atmospheric temperature due to phytoplankton light absorption.

Marine biota and phytoplankton play a major role in the absorption of light and therefore in the vertical distribution of heat in the upper layers of the ocean (**?**). Indeed, observational evidence ~~support~~ supports the hypothesis that chlorophyll increases the upper ocean heat uptake. For instance, satellite observations show that phytoplankton blooms can cause an increase of sea surface temperature (SST) of 1.5°C (**?**). Furthermore, previous remote sensing data indicate an increase in local SST of 4.5°C on a 4 day-timescale due to the presence of phytoplankton blooms (**?**). Recent high-resolution in situ observations in the Indo-West Pacific Ocean ~~indicate~~ highlight large anomalies of temperature of 0.95°C in the uppermost skin layer of the ocean when large phytoplankton blooms appear (**?**). However, all these observations are either on a short time scale or in a geographically limited area. To study the larger-scale impact of phytoplankton light absorption and its ~~varying~~ relative magnitude, Earth system models are employed.

~~Different models with different~~ Models of differing complexity are used to study the effect of phytoplankton light absorption. For instance, using ocean-only (**?**) or general circulation models~~(???)~~ , several studies focusing on the tropical Pacific Ocean (???) or on the Arctic Ocean (**?**) report an increase of SST between 0.5-2°C ~~. The same magnitude of ocean warming is reported with a general circulation model focusing on the Arctic Ocean (?). These changes in ocean temperature have an impact on the nutrient availability and the biogeochemical properties of the ocean (??).~~ due to phytoplankton light absorption. A warming of the ~~surface of the ocean~~ ocean surface induced by marine biota ~~also~~ has consequences on the overall climate system. For instance, **?** find that an increase of SST due to phytoplankton light absorption increases the atmospheric humidity content thereby increasing the greenhouse effect and the atmospheric temperature locally by up to 0.5°C. Furthermore, phytoplankton can amplify locally the seasonal ~~cycle~~ temperature of the lowest atmospheric layer ~~temperature by 1K (?). Moreover, ? indicate that the climate effect of phytoplankton can even extend through the troposphere in mid-latitude regions, influencing the~~ by 1°C, changing the Walker and Hadley circulation (**?**).

It is therefore known that phytoplankton light absorption has a non-negligible role on the atmospheric temperature but which climate ~~pathways are~~ pathway is the most important behind this warming is still unclear. Phytoplankton light absorption affects the surface atmospheric temperature via two climate pathways. First, various modeling studies suggest that biologically-induced surface water heating can increase the air-sea heat exchange (**???**) with consequences on the formation of tropical storms and monsoons in the Arabian Sea (**?**). Second, the solubility of gases and thus also the air-sea CO_2 exchange is affected by phytoplankton light absorption. For instance, **?** study the impact of this biogeophysical mechanism on the air-sea flux of CO_2 and find that phytoplankton light absorption has a small outgassing effect on a global scale with high regional fluctuations.

However, none of these studies have analyzed, disentangled and compared the changes in both air-sea heat and CO_2 exchange due to phytoplankton light absorption. To shed light on the biologically-induced atmospheric warming, we use a recent Earth

system model ~~of intermediate complexity (?). The model is called EcoGENIE (?)where~~ called EcoGEnIE (?). In a earlier study, we implemented phytoplankton light absorption in ~~an earlier study~~ this model (?). We ~~use the same model setup to determine how the importance of this biogeophysical mechanism on biologically-induced atmospheric warming. We conduct several simulations to determine the importance of the climate pathways behind the atmospheric warming. We~~ consider two different biologically-induced changes: ~~a change~~ changes in air-sea heat and changes in air-sea CO_2 exchange ~~rates~~ (Fig. 1). The air-sea CO_2 exchange can be influenced by the dissolved oceanic CO_2 in ~~the ocean in~~ three different ways: through 1) ~~the biological pump~~ changes in the biogeochemical pumps as a result of phytoplankton light absorption~~that affects the marine biogeochemical cycles (??),~~ . For instance, ? have shown that changes in oceanic circulation due to phytoplankton light absorption enhance the vertical supply of nutrients, increasing the relative abundance of calcifiers. As a consequence, the primary production and the export production of organic matter increase. Through 2~~) the solubility of~~) decrease in CO_2 ~~due fluctuations of SSTand~~ solubility due to higher SST, increasing the atmospheric CO_2 concentrations and the greenhouse gas effect. Through 3) decrease in sea-ice formation ~~and resulting~~ because sea-ice ~~extent altering the air-sea CO_2 flux~~acts as an ocean cap that blocks gas exchanges.

~~The paper is organized as follow: In section 2, we describe the components of the model, the light absorption scheme and the air-sea exchanges. In section 3, we describe the simulations and the modeling strategy. In section 4, we report several sensitivity analyses of the climate system with EcoGENIE. In section 5, we present our results and detail the changes in both oceanic and atmospheric properties. In section 6, we conclude by commenting on the role of this biogeophysical mechanism in the atmospheric warming.~~

2 Model description

Our motivation is to study the interactions between the marine ecosystem, the biogeochemistry, the biogeophysics and the climate system. These interactions are computationally expensive in high-resolution models therefore we used an Earth system model of intermediate complexity (?). The Earth system model employed is the ~~Grid-ENabled~~ carbon-centric Grid-Enabled Integrated Earth system model (~~GENIE) (?) composes~~ cGEnIE) (?) composed of several modules describing the dynamics of the Earth system (Fig. 2). This model has been previously calibrated and compared to observations ~~several times (????). GENIE (????).~~ Moreover, this model is widely used to study past climate and changes in the carbon cycle over geological times ~~(??). Furthermore, GENIE has been used to demonstrate that~~ (???), past mass extinctions (?) and biogeochemistry processes (?). Additionally, cGEnIE is employed to assess the sensitivity of atmospheric CO_2 ~~is mainly explained~~ to biogeochemical pumps, ocean circulation and climate feedbacks (?). The authors explain the variance of atmospheric CO_2 by the organic carbon pump~~(?). We use the carbon-centric version (cGENIE) that has been previously employed to study past mass extinction (?), the climate system (?) or biogeochemistry processes (?). GENIE is associated with the~~ , arising from changes in the Southern Ocean deep convection which brings more dissolved inorganic carbon (DIC) to the surface. A new ecosystem component

(ECOGEM) is associated with cGEnIE to form the recent ~~EcoGENIE~~ EcoGEnIE model (**?**). ~~EcoGENIE has been~~ EcoGEnIE is used to determine the link between the marine plankton ecosystem and various past climate scenarios (**?**) with focus on phosphorus inventory (**?**). For our study, the model combines different components including ocean hydrodynamics, atmosphere, sea-ice, ocean biogeochemistry and marine ecosystem component. ~~The efficient numerical terrestrial scheme (?) is not used in this study, so~~ We do not consider a terrestrial component meaning that the land surface is essentially passive. We use the same configuration as described in detail by **?** and ~~thus only briefly explain the individual model components~~the following description only refers to our specific model setup.

2.1 Modules

2.1.1 The physical components

The physics of the model contains a frictional-geostrophic ocean circulation (GOLDSTEIN), coupled to a 2D energy-moisture balance model of the atmosphere (EMBM) and a thermodynamic sea-ice model (GOLDSTEINSEAICE) (**??**). Heat and moisture are exchanged between the three components and act as a coupling strategy.

The oceanic component calculates the horizontal and vertical redistribution of heat, salinity and biogeochemical elements via advection, convection and mixing. The ocean module is configured on a 36×36 horizontal grid. The horizontal grid is uniform in longitude and uniform in sine latitude, giving $\sim 3.2^\circ$ latitudinal increments at the equator increasing to 19.2° in the highest latitude. This horizontal grid has been used for previous biogeochemical simulations (**??**). We consider 32 vertical oceanic layers increasing logarithmically from 29.38 m for the surface layer to 456.56 m for the deepest layer. This vertical resolution ~~has already been~~ is already used to study the relative importance of biogeophysical and biogeochemical mechanisms on the climate system (**?**).

The atmospheric component is based closely on the UVic Earth system model (**?**). The prognostic variables are atmospheric temperature and specific humidity. Precipitation removes instantaneously all moisture corresponding to an excess above a relative humidity threshold. The wind stress is prescribed and identical between all simulations, the temperature cannot affect the wind stress.

The sea-ice component solves the equation for part of the ocean covered by sea-ice. The prognostic variables are ice thickness and ice areal fraction. The transport of sea-ice includes sources and sinks of these variables. The growth or decay of sea ice depends on the net heat flux into the ice. The dynamics in this module consist of advection by currents and diffusion. Sea-ice doesn't limit the penetration of photosynthetically available radiation in the ocean.

2.1.2 Ocean biogeochemistry component

The biogeochemical module (BIOGEM) represents the transformation and spatial redistribution of biogeochemical tracers (**?**). The state variables are inorganic ~~resources~~ and organic matter. The biological uptake is represented by an implicit biological community: nutrients are directly converted into organic matter via an uptake rate. The biological uptake is limited by light, temperature and nutrient availability. Organic matter is partitioned into dissolved and particulate phases (DOM and POM).

~~The model~~ For this study, BIOGEM does not consider a temperature dependency on iron solubility and iron bioavailability. Our model setup includes iron (Fe) and phosphate (PO_4) as limiting nutrients. Similar to **?**, we do not consider nitrate ~~(NO_3^-) here.~~ here. Moreover, the surface production is redistributed in the water column as a depth-dependent flux. To achieve this, the surface export is divided between refractory organic matter remineralised close to the seafloor and labile organic matter remineralised in the upper water column (**?**). Furthermore, because we do not consider a sediment component, all organic matter reaching the sea-floor is instantaneously remineralised. Calcium carbonate ($CaCO_3$) is represented in the model and its dissolution below the surface is treated as the remineralization of POM. Recent studies have implemented and calibrated a temperature-dependent remineralization in the the model (**??**) but this parameterization is not included in our model setup. Furthermore, BIOGEM calculates the air-sea CO_2 and O_2 exchange. The value of atmospheric CO_2 predicted by BIOGEM is used as input for the radiative scheme of the atmospheric component, thus providing climate feedback.

2.1.3 Ecosystem component

The marine ecosystem component (ECOGEM) represents the marine plankton community and associated interactions ~~in~~ within the ecosystem (**?**). The biological uptake in ECOGEM replaces the BIOGEM uptake calculation and is limited by light, temperature and nutrient availability. Plankton biomass and organic matter are subject to processes such as resource competition and grazing before being passed to DOM and POM. Several ecophysiological parameters are size-dependent such as: maximum nutrient uptake rate, cell carbon quotas, grazing and partitioning between DOM and POM. Additionally, the nutrient uptake, photosynthesis and predation are temperature-dependent. The ecosystem is divided into different plankton functional types (PFTs) with specific traits. ~~Furthermore, each~~ Each PFT is sub-divided into size classes with specific size-dependent traits. ~~We consider two classes of~~ Here, we consider only two PFTs: phytoplankton and zooplankton (Appendix A1). Phytoplankton is characterized by nutrient uptake and photosynthesis whereas zooplankton is characterized by predation traits. Zooplankton grazing depends on the concentration of prey biomass~~availability~~, with predominantly grazing on ~~preys~~ prey that are 10 times smaller than themselves. Each population is associated with biomass state variables for carbon, phosphate, iron and chlorophyll. The production of dead organic matter is a function of mortality and messy feeding, with partitioning between non-sinking dissolved and sinking particulate organic matter. Finally, plankton mortality is reduced at very low biomass such that plankton cannot become extinct.

2.2 Light absorption in the ocean

~~The implementation of phytoplankton light absorption in EcoGENIE is the same as the scheme described in ? and~~ In the previous model version (**?**), light was only absorbed by phytoplankton. In the model version of **?**, a new light scheme is implemented where the absorbed light by phytoplankton is converted into heat and is able to affect the oceanic temperature. Furthermore, light absorption takes place throughout the water column and is not restricted to the first oceanic layer anymore. The same light absorption scheme is a coupling between Eq. 1 and Eq. 2. For ~~a simplification issue~~simplicity, in our model configuration, the incoming shortwave radiation does not vary seasonally. We look at long-term changes in the climate system therefore the absence of a seasonal cycle does not affect ~~our results~~ the overall qualitative and main findings. The presence of or-

ganic, inorganic particles and dissolved molecules restrains the light penetration in the ocean (**?**). The vertical light attenuation scheme is given by Eq.1:

$$I(z) = I_0 \cdot \exp(-k_w - k_{Chl} \cdot Chl_{tot}) \cdot z \tag{1}$$

where $I(z)$ is the irradiation of the full solar spectrum at depth z, I_0 is the irradiation at the surface of the ocean, k_w is light absorption by clear water and inorganic particles (0.04 m^{-1}), k_{Chl} is the light absorption by chlorophyll (0.03 m^{-1}(mg Chl)$^{-1}$) and $Chl_{tot}(z)$ is the ~~total chlorophyll concentration~~ chlorophyll concentration at depth z. The values for k_w and k_{Chl} are taken from **?**. The parameter I_0 is negative in the model because it is a downward flux from the sun to the surface of the ocean. We allow primary production and light to penetrate until the sixth layer of the model (221.84 m deep), which is the lower limit of the euphotic zone (**?**). In our model setup, maximum absorption occurs in the upper oceanic layer and minimum absorption occurs in the sixth layer.

Phytoplankton changes the optical properties of the ocean (**?**) through phytoplankton light absorption. Therefore it can cause a radiative heating and change the oceanic temperature. We implemented phytoplankton light absorption into the model following **?** and **?**. The scheme is give by Eq.2:

$$\frac{\partial T}{\partial t} = \frac{1}{\rho \cdot c_p} \frac{\partial I}{\partial z} \tag{2}$$

$\partial T/\partial t$ denotes the temperature changes, c_p is the specific heat capacity of water, ρ is the ocean density, I is the solar radiation incident at depth z. Part of the light absorbed is used by phytoplankton for photosynthesis and part ~~is released in form of fluorescence and heat. However, the fluorescence form can be ignored, therefore it is assumed that the whole light absorption~~ leads to heating of the water~~(?)~~.

2.3 Air-sea heat exchange

~~Heat is exchanged between the atmosphere, the ocean and the sea-ice components and acts as a coupling between these three modules.~~ We detail here ~~only the relevant fluxes for our study, the heat flux~~ the total heat flux from the ocean and sea-ice going into the atmosphere. The vertically integrated atmospheric heat equation (Eq. 3) is given by **?** and **?**~~Eq. 3~~:

$$Q_{ta} = Q_{SW} \cdot C_A + Q_{LH} + Q_{LW} + Q_{SH} - Q_{PLW} \tag{3}$$

Q_{ta} corresponds to the total heat flux into the atmosphere, Q_{SW} is the net shortwave radiation corresponding to the solar irradiance ~~receives~~ received from the sun and reflected by the planet's albedo, C_A is a heat absorption coefficient (0.3 over the ocean ~~, ?~~(?)), Q_{LH} is the latent heat flux corresponding to phase change of a ~~certain~~ thermodynamic system, Q_{SH} is the sensible heat flux corresponding to temperature change of a thermodynamic system, Q_{LW} is the net (upward minus downward) re-emitted longwave radiation corresponding to infrared energy coming from the planet and Q_{PLW} is the outgoing planetary

longwave radiation.

The atmosphere loses heat through net longwave radiation, dominated by the outgoing longwave radiation, thus the total longwave heat flux (Q_{LW} + Q_{PLW}) is negative in the model. Furthermore, evaporative cooling of the ocean leads to a latent heat release in the atmosphere upon condensation and precipitation. Evaporated water vapour may be transported away from an oceanic source, to condense and precipitate elsewhere.

2.4 Air-sea CO_2 exchange

The atmospheric temperature depends on the atmospheric CO_2 concentration which is affected by the transfer of CO_2 between the ocean and the atmosphere. The flux of CO_2 across the atmosphere-ocean interface (Eq. 4) is given by **?**~~Eq. 4~~:

$$F_{CO_2} = k \cdot \rho \cdot (C_w - \alpha \cdot C_a) \cdot (1 - A) \tag{4}$$

F_{CO_2} is the air-sea CO_2 flux, k corresponds to the gas transfer velocity, ρ is the ocean density, C_w is the concentration of dissolved gas in the surface ocean, α is the solubility coefficient calculated from **?** and depends on the sea surface temperature and salinity, C_a is the concentration of gas in the atmosphere and A is the fraction of the ocean covered by sea-ice.

Phytoplankton light absorption ~~affects the~~ warms the surface of the ocean and thus reduces CO_2 solubility and sea-ice fraction. The flux of CO_2 is therefore affected via the parameters C_w, α and A. To study precisely the flux we either prescribe these parameters in the air-sea CO_2 exchange calculation or let them evolve freely ~~. To prescribe these parameters we take the values from the reference run~~ (see below).

3 Model setup and simulations

During this study, we are ~~mainly~~ primarily interested in the relative differences between our selected simulations. We focus on the relative impact of phytoplankton light absorption on different climate pathways rather than on the changes in the climate state. We try to simulate a realistic mean climate system but the absolute value of the climate quantities are less relevant due to the limitations of such ~~an intermediate complexitymodel~~a model of intermediate complexity.

For a realistic nutrient distribution in the ocean, we performed a BIOGEM spin-up for 10,000 years. During the spin-up the atmospheric CO_2 concentration is fixed to 278 ppm. The simulations restart for 1,000 years after the spin-up with ECOGEM, meaning that all simulations consider marine biota. ~~The model setup~~Due to the single layer atmospheric component, the non-seasonality and the non-representation of the land dynamics, running the model for 1,~~ecosystem community and grid resolution employed are the same~~ 000 years is sufficient to achieve steady-state. The results represent the annual mean of the last year of the simulations, when the model is in steady-state. The present-day continental configuration, model setup, grid resolution and ecosystem community are identical as in **?**. For simplification, only one phytoplankton and one zooplankton species are included in the model setup (Appendix A1 ~~) except that we run the model without any seasonal cycle~~and B1). The seasonal cycle is removed for technical issues, we cannot prescribe the seasonal cycle of SST but only the annually-averaged

SST. The absence of the seasonal cycle is not an issue for this study because we look at the importance of each climate pathway rather than focusing on the quantitative changes of the climate system.

The carbon cycle is closed in our simulations, meaning that there is no input of carbon through volcanic or anthropogenic activities. Only the size of the carbon reservoirs can vary. If not stated otherwise, the concentration of atmospheric CO_2 evolves freely in the simulations. ~~Furthermore, all~~ All simulations are forced with the same constant flux of dissolved iron into the ocean surface (**?**).

~~To study the~~ To ensure that the model is suitable for our study, we conducted two sensitivity analyses. First, we analyzed the climate sensitivity of the model by conducting two simulations with different atmospheric CO_2 concentrations (Appendix C1). Second, we ensure that the heat and CO_2 interaction is negligible (Appendix D1). To study the effect of phytoplankton light absorption on the atmospheric temperature we perform seven different simulations, all including the ECOGEM component (Fig. 3~~; Table **??**):~~):

- ~~The first one, called~~ *Bio* is the reference run and is the only simulation that does not include phytoplankton light absorption (k_{Chl} = 0 in Eq. 1). In this simulation, all the climate pathways evolve freely.

- ~~The second one, called~~ *BioLA* is the same as the reference run but ~~with~~ phytoplankton light absorption is implemented. In this simulation, all the climate pathways evolve freely.

- ~~The third simulation~~ *HEAT* is the same as the second one except that we prescribe the atmospheric CO_2 concentration only for the atmospheric temperature calculation. For a comparison with the reference run, the prescribed atmospheric CO_2 concentration from *Bio* is used (169 ppm). The effect of CO_2 on atmospheric temperature is fixed but the air-sea heat fluxes evolve freely. This simulation ~~determines~~ analyses the effect of phytoplankton-induced changes of air-sea heat ~~flux on the energy budget~~fluxes on the atmospheric temperature.

- ~~The fourth simulation is named~~ *CARB* ~~where we run the model~~ is the simulation with an uncoupled ocean-atmosphere setup. The atmospheric component is forced with the heat fluxes from ~~the reference run~~ *Bio* and the atmospheric CO_2 concentration is prescribed with the value of *BioLA*. This simulation determines the effect of phytoplankton-induced changes of atmospheric CO_2 concentration on the atmospheric temperature. Please note that *CARB* is well suited for studying the atmosphere properties but not to examine ocean dynamics.

- ~~The fifth simulation is named~~ *HCorg* ~~and~~ where we only allow the ~~biological pump~~ biogeochemical pumps (soft-tissue pump and carbonate pump) to affect the dissolved CO_2. The solubility of CO_2 (α in Eq. 4) and sea-ice extent (A in Eq. 4) parameters are prescribed using the respective values from *Bio*. The CO_2 solubility is fixed by prescribing the SST only for this calculation. In *HCorg* air-sea heat exchange and the ~~biological pump~~ biogeochemical pumps parameter (C_w in Eq. 4) evolve freely.

- ~~The sixth simulation is called~~ *HCorgSI* where the ~~biological pump~~ biogeochemical pumps and sea-ice extent affect dissolved CO_2. The ~~solubility of the~~ CO_2 ~~parameter~~ solubility (α in Eq. 4) is prescribed using the value of *Bio*. In

HCorgSI the air-sea heat exchange, the ~~biological pump~~ biogeochemical pumps (C_w in Eq. 4) and sea-ice extent (A in Eq. 4) parameters evolve freely.

- ~~The seventh and last simulation is called~~ *HCorgSol* where the ~~biological pump~~ biogeochemical pumps and the solubility pump affect dissolved oceanic CO_2 ~~in the ocean~~. The sea-ice extent parameter (A in Eq. 4) is prescribed using the value of *Bio*. In *HCorgSol* the air-sea heat exchange, the ~~biological pump~~ biogeochemical pumps (C_w in Eq. 4) and the CO_2 solubility (α in Eq. 4) parameters evolve freely.

4 ~~Sensitivity analysis~~

3.1 ~~Climate variability~~

~~To analyze the climate variability of the model, we perform two sensitivity analyses (Table **??**). Both simulations have the same model setup, restart from the spin-up described previously but their atmospheric CO_2 concentration differ. The first simulation (Sensi280) has an atmospheric CO_2 concentration of 280 ppm while the second one (Sensi320) has an atmospheric CO_2 concentration of 320 ppm. Furthermore, the simulations Sensi280 and Sensi320 consider phytoplankton light absorption.~~

~~An increase of 40 ppm in atmospheric CO_2 concentration slightly reduces the chlorophyll concentration but these changes are negligible. The oceanic and atmospheric heat budgets are affected by the changes in atmospheric CO_2 concentration. Increasing the greenhouse gas concentrations increases in turn the SAT and therefore the SST due to the exchange of heat between the ocean and the atmosphere.~~

3.1 ~~Air-sea fluxes interactions~~

~~To estimate the unique effect of each climate pathway we ensure that the heat and CO_2 interaction is negligible. Due to the model setup, the flux of CO_2 across the air-sea interface (F_{CO_2}; Eq. 4) depends on the SST via the Schmidt number (**??**). We conduct two comparable sensitivity analysis and analyze the changes in F_{CO_2}. First, we artificially increase the SST by 1°C and do not exceed the maximum difference of SST between our simulation results (Table **??**). This increase in SST only enhances F_{CO_2} by $4.26 \cdot 10^{-5}$ mol/m^2/yr, representing a raise of 2.58% of the total air-sea CO_2 exchange. Even large SST fluctuations negligibly affect the flux of CO_2 at the air-sea interface. Second, the mean wind speed affects the F_{CO_2} via the gas transfer velocity (k; Eq. 4). We increase the wind speed by 0.2 m/s, which is a comparable forcing of the artificial increase of 1°C of SST (**?**). This increase in mean wind speed enhances the F_{CO_2} by $1.44 \cdot 10^{-4}$ mol/m^2/yr, representing an increase of 8.69% of the total air-sea CO_2 flux. Clearly, the changes in wind speed are much larger than the changes in SST hence we consider that the effect of SST on the air-sea CO_2 exchange is small enough to be neglected.~~

4 Global response of the climate system

In this section we present the results of the simulations on a global scale~~, we~~ . We do not consider local patterns because we removed any seasonal cycle in our model setup. ~~As already mentioned, the absence of the seasonal cycle is not an issue for our study because we focus on the importance of each climate pathway rather than analyzing the quantitative assessments of the climate pathways~~Moreover, the horizontal grid resolution is low and marine biota cannot move between grid cells, thus even if seasonality was included, key regional patterns will not be resolved. First, we focus on the chlorophyll biomass and sea surface temperature because phytoplankton light absorption has a direct effect on these climate variables (**???**). Second, these changes in oceanic properties affect the carbon cycle (**??**), therefore we study the changes in atmospheric CO_2 concentration~~between the simulations~~. Third, phytoplankton light absorption alters the atmospheric properties (**?**), thus we analyze the changes in radiative heat fluxes, humidity and evaporation~~between the simulations~~. Finally, ~~due to changes in oceanic and atmospheric properties,~~ the response of the surface atmospheric temperature is ~~studied~~analyzed.

4.1 Chlorophyll biomass and sea surface temperature

Our results indicate differences of ~~sea surface temperature (SST)~~ SST and chlorophyll biomass, depending on the climate pathways included in our model setup (Table 1). Due to the uncoupled ocean-atmosphere setup in *CARB*, ocean dynamics are not presented in this section. The reference run *Bio* has the lowest chlorophyll biomass and a low SST while the simulation *BioLA* has the highest chlorophyll biomass and SST. ~~As previously demonstrated~~The increase in chlorophyll biomass is due to two different mechanisms: First, phytoplankton light absorption ~~increases the chlorophyll biomass and therefore the SST via shallower downward flux of organic matter and higher~~ leads to a higher surface production, enhancing the remineralization at the surface of the ocean as shown by **?**. Second, phytoplankton light absorption enhances the upward vertical velocity. As a result of these two mechanisms, the surface nutrient concentrations ~~(??). The chlorophyll biomass difference~~ increase, explaining the higher chlorophyll biomass. The increase in surface chlorophyll biomass due to phytoplankton light absorption between *BioLA* and *Bio* is 0.012 mgChl/m^3~~which is in agreement with previous estimates (??). However, the~~ , in line with a previous estimate of 0.014 mgChl/m^3 (**?**). The higher chlorophyll biomass is, however, limited by the increase in zooplankton biomass applying a top-down control. Via the effect of phytoplankton light absorption, a higher surface chlorophyll biomass leads to an increase of SST. The global difference of SST between *BioLA* and *Bio* ~~of only~~ is of 0.08°C. This value is lower than previous ~~estimates (???)~~model estimates that show a global SST increase of 0.45-1°C due to phytoplankton light absorption (**???**). This underestimation of the biologically-induced SST heating is due to the non-seasonal radiative forcing of the model~~. The non-seasonal radiative forcing decreases~~ , decreasing the global heat budget (Appendix E1)~~, explaining the lower response of the SST in our study~~.

~~The~~ In *HEAT*, the chlorophyll biomass is higher while the SST is lower ~~in *HEAT* compared to the reference simulation~~ compared to *Bio* (Table 1). This is rather counter-intuitive and is due to changes in oceanic circulation between these two simulations. For instance, the maximum Atlantic ~~overturning circulation~~ meridional overturning circulation (AMOC) is 8.6

Sv in *HEAT* while it is 7.6 Sv in *Bio*. ~~The stronger overturning~~ In *HEAT*, the SST is lower and the sea-ice cover is slightly higher (Appendix F1) compared to *Bio*, leading to more deep water formation in polar latitudes. As a result, the AMOC is enhanced in *HEAT*. The stronger oceanic circulation in *HEAT* ~~increases the concentration of surface nutrients. Specifically~~ leads to an enhanced nutrient redistribution, thus increasing the surface nutrient concentrations. For instance, the surface PO_4 concentration is ~~about~~ ~0.21 μmol/kg in *HEAT* while it is ~~about~~ ~0.19 μmol/kg in *Bio*. The higher surface PO_4 concentration in *HEAT* explains the higher chlorophyll biomass in this simulation compared to ~~the reference simulation. The changes in the strength of the circulation explain as well the lower SST in *HEAT* compared~~ *Bio*. The ~~stronger~~ enhanced oceanic circulation in *HEAT* compared to *Bio* leads to a ~~more important~~ stronger redistribution of heat along the water column, explaining the surface cooling and the warming of the ~~bottom water~~deep ocean in *HEAT*. Our results indicate that the bottom water temperature in *HEAT* is 3.57°C while it is 3.09°C in *Bio*.

The ~~simulation~~ surface chlorophyll biomass in the simulations *HCorg*, *HCorgSI* and *HCorgSol* ~~have a higher chlorophyll biomass and SST than the reference run. Furthermore, the chlorophyll biomass and the SST are similar between the simulation~~ are higher than the surface chlorophyll biomass in *Bio* due to the higher surface PO_4 concentrations. In *Bio* the surface PO_4 concentration is 0.18 μmol/kg while in the simulations *HCorg*, *HCorgSI* and *HCorgSol* the surface PO_4 concentrations are >0.21 μmol/kg. The higher surface PO_4 concentrations are due to enhanced remineralization at the ocean surface and enhanced upward vertical velocities. Due to the effect of phytoplankton light absorption, the higher surface chlorophyll biomasses in *HCorg*, *HCorgSI* and *HCorgSol* lead to higher SSTs compared to *Bio*. Only the sea-ice extent differs between the simulations *HCorg* and *HCorgSI* ~~indicating that the changes in~~ but their chlorophyll biomass and SSTs are identical. This result evidences a lack of sea-ice ~~extent due to phytoplankton light absorption do not affect~~ influence on these climate variables ~~(Appendix F1)~~and thus on the heat fluxes. In addition, the chlorophyll biomass and SST are higher in *HCorg* ~~than in~~ compared to *HCorgSol*, indicating that the solubility factor has a negative ~~feedback~~ effect on these climate variables. Between these two simulations, the only difference is the CO_2-solubility factor that can evolve freely in *HCorgSol*. In the simulation *HCorg*, the SST for the calculation of the ~~solubility of~~ CO_2 solubility is prescribed using the ~~values of the reference run. The SST in the reference run is lower than the SST in *HCorgSol*~~value of *Bio*, which is the lowest value. Considering the physical and chemical properties of the ocean, a low SST increases the solubility of CO_2 (**?**). Therefore, the CO_2 solubility is reduced in *HCorgSol* compared to *HCorg*, due to the higher SST in *HCorgSol*. For instance, our results indicate that on a global scale, the surface oceanic CO_2 concentration is 27.200 μmol/kg in *HCorgSol* while it is 27.213 μmol/kg in *HCorg*. ~~These~~ Via the nutrient ratios, these changes in carbon cycle between the simulations affect the ~~others biogeochemical cycles via the nutrient ratios~~ phosphate and iron cycles (**?**). As a consequence, the surface PO_4 concentration is ~~about~~ ~0.216 μmol/kg in *HCorg* and about ~0.214 μmol/kg in *HCorgSol*. The higher surface PO_4 concentration ~~at the surface in *HCorg* leads to the higher~~ leads to a larger surface chlorophyll biomass and higher SST ~~due to phytoplankton light absorption~~ in *HCorg* compared to *HCorgSol*.

4.2 Atmospheric properties

The oceanic properties differ between the simulations, thus we expect differences ~~between~~ in the atmospheric properties~~in each simulation. First, we~~ . We compare the atmospheric CO_2 concentration, ~~then~~ the heat fluxes, the evaporation, the specific humidity and finally the surface atmospheric temperature between the simulations.

4.2.1 Atmospheric CO_2 concentration

The atmospheric CO_2 concentrations for the simulations is low compared to the pre-industrial level (Fig. 4). This is due to our new model setup that allows primary production until the sixth oceanic layer, meaning that more carbon is stored in the deep ocean, reducing the atmospheric CO_2 concentration (see **?**). In all the simulations considering phytoplankton light absorption, the atmospheric CO_2 concentration is higher than in the reference run~~(Table ??).~~ . In a previous study, we evidence that the higher atmospheric CO_2 concentration is mainly due to decrease in CO_2 solubility via the higher SST while the enhanced remineralization of organic matter and the dissolution of $CaCO_3$ slightly affect the atmospheric CO_2 concentration (**?**). The atmospheric CO_2 concentration is the lowest in *Bio* while it is the highest in *BioLA*, with a difference of 9 ppm. ~~The difference of CO_2 concentration between the simulations *BioLA* and *Bio*~~ This value is lower than ~~previous estimate (?) and~~ a previous estimate that indicates an increase of atmospheric CO_2 concentration of 18 ppm (**?**). This lower estimate is due to the non-seasonal cycle forcing~~(Appendix E1). As already described in ?, the higher atmospheric~~ , neglecting the seasonal variations of air-sea CO_2 ~~concentration in *BioLA* is mainly explained by lower CO_2 solubility due to a higher SST~~exchanges.

In *HEAT*, the atmospheric CO_2 concentration is prescribed only ~~in~~ for the atmospheric temperature calculation~~, therefore~~ . Therefore the atmospheric CO_2 concentration can vary due to changes in dissolved oceanic CO_2, ~~solubility and~~ sea-ice extent ~~, and therefore affect~~ and CO_2 solubility, affecting the other climate variables. The atmospheric CO_2 concentration in *HEAT* is slightly higher than in *Bio*. ~~The chlorophyll biomass is more important~~ This is due to the larger chlorophyll biomass in *HEAT* than in ~~the reference simulation~~*Bio* (Table 1), indicating a higher ~~amount of organic matter and therefore a more important remineralization rate~~ production and thus more remineralization in the ocean. During the remineralization process, CO_2 is produced~~(?), therefore~~ , thus the higher remineralization ~~rate~~ in *HEAT* increases the dissolved CO_2 concentration. On a global scale, our results indicate that the surface dissolved oceanic CO_2 is about 6.354 mol/kg in *HEAT* while it is 6.302 mol/kg in ~~*BIO*~~*Bio*. The ~~more important dissolved~~ larger dissolved oceanic CO_2 concentration in *HEAT* increases the air-sea CO_2 flux and ~~therefore~~ in turn the atmospheric CO_2 concentration (see Eq. 4).

The atmospheric CO_2 concentration in *CARB* is similar to the one in *BioLA* because we prescribed the value against the one in *BioLA*.

The simulations *HCorg*, *HCorgSI* and *HCorgSol* have a higher atmospheric CO_2 concentration than ~~the reference run~~in *Bio*. This is again not surprising because these simulations consider phytoplankton light absorption which ~~increase~~ increases the

atmospheric CO_2 concentration ~~(?)~~as shown by **?**. The atmospheric CO_2 concentration between *HCorg* and *HCorgSI* is similar ~~due to the similar~~ even if their sea-ice extent and sea-ice thickness differs (Appendix F1)~~and~~ . The changes in sea-ice ~~thickness, the sea-ice does~~ do not have an ~~impact~~ effect on the atmospheric CO_2 concentration. The slightly higher atmospheric CO_2 concentration in *HCorgSol* compared to *HCorg* is due to changes in CO_2 solubility~~between these two simulations.~~ : As described above, the CO_2 solubility is lower in *HCorgSol* compared to *HCorg*. As a consequence, the air-sea CO_2 flux is higher in *HCorgSol* compared to *HCorg*, leading to a slightly higher atmospheric CO_2 concentration in *HCorgSol*~~(Eq. 4).~~ .

4.2.2 Heat fluxes

The air-sea heat flux is divided into the net shortwave radiation, the net re-emitted longwave radiation, the sensible heat flux and the latent heat flux (Fig. G). The ~~simulations *HCorg* and *HCorgSI* have exactly the same heat fluxes because these simulations are identical in all points (Appendix F1). Furthermore, the simulations~~ air-sea heat fluxes represent the total heat fluxes from the ocean and sea-ice, going into the atmosphere. The simulations ~~*BioLA*~~*HCorg* and ~~*HCorgSolalso have*~~ *HCorgSI* have exactly the same heat fluxes. The only difference between these two simulations is the ~~prescribed and~~ different sea-ice extent for the calculation of the air-sea CO_2 flux. This change in air-sea CO_2 flux does not alter the air-sea heat flux, explaining the identical radiative heat fluxes between *HCorg* and *HCorgSI*. Furthermore, the simulations *BioLA* and *HCorgSol* have the same heat fluxes and the only difference is also the sea-ice extent. As detail previously, the changes in sea-ice extent do not affect the heat fluxes, explaining the identical radiative fluxes between *BioLA* and *HCorgSol*. Finally, the heat fluxes between *CARB* and *Bio* are identical because we prescribed the heat fluxes in *CARB* with the values of *Bio*.

The net shortwave heat flux is divided in two fluxes: the incoming shortwave radiation from the sun entering the atmosphere and the outgoing reflected shortwave radiation leaving the atmosphere. Figure Ga shows that the net shortwave heat flux is identical for all the simulations and is positive. The positive values indicate that net shortwave heat flux is dominated by the flux entering the system, the incoming radiation. The incoming shortwave radiation from the sun is always identical between simulations~~, therefore~~ . Therefore identical net shortwave heat flux implies that the outgoing reflected shortwave radiation is as well the same between simulations due to the treatment of shortwave radiation in the ~~atmosphere given by ?~~model (**?**).

The net longwave heat flux is negative for all simulations~~pointing out~~ , indicating that this flux is dominated by the upward longwave radiation leaving the atmosphere (Fig. Gb). A ~~higher~~ more negative value of net longwave heat flux indicates a ~~higher~~ greater loss of heat ~~in~~ to outer space. The simulations *Bio* and *CARB* have the ~~highest~~ least negative net longwave heat flux while ~~the simulation~~ *HEAT* has the ~~lowest~~ highest negative heat flux, indicating that ~~the simulation~~ *HEAT* loses more heat than the others simulations. The higher heat loss in ~~the simulation~~ *HEAT* is due to the lowest SST and a reduced amount of greenhouse gases, precisely a low specific humidity (~~Table ??~~Fig. 6) and atmospheric CO_2 concentration (~~Table ??~~Fig. 4). The lower amount of greenhouse gases in the atmosphere permits a higher loss of heat outside the atmosphere. All the simulations considering phytoplankton light absorption, except *CARB* where the heat fluxes are prescribed, have a higher negative net longwave heat flux compared to *Bio*~~, which is rather~~ . This result is predictable because this biogeophysical mechanism is an

additional heat source for the surface of the ocean, where air-sea heat exchanges occur.

The sensible heat flux depends on the atmospheric and oceanic temperature (**??**). The sensible heat flux increases when the atmospheric temperature decreases and when the oceanic temperature increases. For the simulation *HEAT*, the sensible heat flux is the highest (Fig. Gc) because the atmospheric temperature is the lowest (~~Table ??~~Fig. 7). In contrast, the sensible heat flux is the lowest for the simulation *BioLA* because the gradient of temperature between the ocean and the atmosphere is low. The sensible heat flux in *HCorg* and *HCorgSI* are close to the sensible heat flux of ~~the reference run~~ *Bio* because their air-sea temperature gradients are almost similar.

The global mean latent heat flux (Fig. Gd) depends mainly on the global mean precipitation ~~rate~~ (**?**). The ~~precipitation rate between~~ simulation *Bio* has the smaller latent heat flux due to the lowest precipitation in this simulation (Appendix G1). The latent heat flux in *BioLA*, *HCorg*, *HCorgSI* and *HCorgSol* are almost similar ~~(Appendix G1) explaining the similar latent heat fluxes between~~ due to the almost similar precipitations in these simulations. The precipitation ~~rate~~ in *HEAT* is higher than in *Bio*, explaining the higher latent heat flux in *HEAT*. ~~Furthermore, the reference run and *CARB* have the smallest latent heat flux due to the small precipitation rate for these simulations.~~

4.2.3 Specific humidity and evaporation

The specific humidity and the evaporation in *BioLA* and *HCorgSol* are similar and the same is true between the simulations *HCorg* and *HCorgSI* (~~Table ??). Furthermore, the~~ Fig. 6). The specific humidity and evaporation are the lowest in ~~the reference simulation~~ *Bio* due to the lowest latent heat flux in this simulation. Including phytoplankton light absorption ~~changes the heat budget, specifically increasing the~~ increases the latent heat flux and therefore ~~increasing~~ increases the specific humidity and evaporation, which is consistent with ~~??. In~~ **?** and **?**. On a global scale, in *BioLA* the ~~specific humidity increases by 0.5% and the~~ evaporation increases by 0.11%~~compared to the reference run, which~~ , thus enhancing the specific humidity by 0.5%. This latter value is lower than previous ~~values~~ estimates where phytoplankton light absorption raises the specific humidity by 2-6% (**?**). The different ~~estimates between our results and ? may~~ values between our estimates and **?** come from the non-seasonal cycle in our model setup, changing the heat budget and therefore underestimating the specific humidity~~and evaporation rate~~. Moreover, the specific humidity in *HEAT* is lower than in *BioLA* due to the lower latent heat flux in the simulation *HEAT*. The evaporation depends on several ~~pathways~~ processes and one of the most important is the humidity in the atmosphere~~(?), the lower is the humidity the higher is the evaporation rate~~, with lower humidity leading to higher evaporation (**?**). As a consequence, the evaporation is higher in *HEAT* than in ~~the simulation~~ *BioLA*. Furthermore, the specific humidity and the evaporation increase when the atmospheric temperature rises ~~as well (?)~~(**?**). The specific humidity and evaporation ~~is higher in the simulations~~ are higher in *CARB* compared to *BioLA* because the surface atmospheric temperature is higher *CARB* (~~Table ??~~Fig. 7). The specific humidity and evaporation in *HCorg* and *HCorgSI* are slightly lower than in *BioLA* because the latent heat flux in *HCorg* and *HCorgSI* is slightly lower. Once the CO_2 solubility factor is considered (simulation *HCorgSol*), the

values of the specific humidity and evaporation are similar to the values in *BioLA*. This is ~~rather~~ not surprising because the heat fluxes between *HCorgSol* and *BioLA* are identical.

4.2.4 Surface atmospheric temperature

The difference ~~of~~ in atmospheric properties between simulations lead ~~indubitably~~ to changes of the surface atmospheric temperature (Fig. 7~~; Table ??~~). First of all, ~~the reference simulation~~ *Bio* has ~~the lowest~~ a low SAT because it doesn't include the additional heat source coming from the phytoplankton light absorption mechanism. The ~~global difference of SAT between *BioLA* and~~ SAT in *Bio* is ~~0.14~~9.31°C ~~which~~ while the SAT in *BioLA* is 9.45°C which makes a global difference of 0.14°C. This estimate is lower than previous estimates ~~(???). The small difference of SAT compared to previous studies is clearly due to our model setup, with a~~ of 0.2-0.45°C (**??**) due to the non-seasonal ~~solar radiation forcing~~cycle in our model.

The lower SAT in *HEAT* compared to *Bio* is due to several reasons. Even if *HEAT* considers phytoplankton light absorption, we show that the SST in *HEAT* is lower than in ~~the reference run. Furthermore, for~~ *Bio*. For the SAT computation, the atmospheric CO_2 ~~concentration is~~ concentrations are identical between *Bio* and *HEAT*~~and~~. Additionally, the specific humidity ~~is slightly higher~~ only increases by 0.27% in *HEAT* compared to *Bio*. Therefore the greenhouse gas effect between these two simulations is rather similar. However, the global net longwave heat flux decreases by ∼0.2 W/m^2 in *HEAT* due to the lower SST, leading to a cooling of the atmosphere. The combination of these different reasons explains the slightly lower SAT in *HEAT* compared to ~~the reference simulation~~*Bio*.

For the simulation *CARB*, the concentration of greenhouse gases (atmospheric CO_2 and specific humidity) is higher than in *Bio* while the air-sea heat fluxes are identical. As a consequence, more heat is trapped in the atmosphere and the SAT increases by 0.71°C compared to the reference run.

The sea-ice extent ~~and thickness are identical~~ is different between *HCorg* and *HCorgSI* (Appendix F1) ~~, resulting in identical response of the climate system and identical~~but the response of SAT is identical, indicating that with our model setup, the changes in sea-ice extent do not affect the SAT. The specific humidity and the atmospheric CO_2 concentration are slightly higher in *HCorg* ~~compared to *Bio*. This slightly higher greenhouse gas concentration leads to~~ and *HCorgSI*, leading to a small increase ~~in SAT of *HCorg*~~ of SAT compared to *Bio*.

In *HCorgSol* the atmospheric CO_2 concentration and the specific humidity are higher than in ~~the reference simulation~~*Bio*. However, the sensible heat flux and the net longwave heat flux are lower in *HCorgSol*. Even if the greenhouse gases concentrations are higher, the reduced ~~in~~ air-sea heat fluxes lead to a slight decrease in SAT in the simulation *HCorgSol* compared to *Bio*.

5 Limitations

To study how phytoplankton light absorption alters the surface atmospheric temperature via air-sea heat and CO_2 exchange, we use the ~~EcoGENIE~~ EcoGEnIE model (**?**). Our study is designed to understand the climate pathways behind the phytoplankton-induced atmospheric warming but our model setup has limitations. Most notably, we do not consider a seasonal cycle in our study. Enabling seasonality would lead to larger seasonal increase of temperature but it would also lead to larger seasonal decrease in CO_2 solubility. Therefore, we don't think that the heat-pathway would overrule the CO_2-pathway. This study investigates the impact of short-lived seasonal organisms, thus having an annual mean approach underestimates the effect of phytoplankton light absorption on the climate system. The absence of nitrogen cycle could have additional effects that are not included in our study. Phytoplankton light absorption warming low-oxygen regions causes an additional oxygen consumption. As a consequence, the denitrification would increase nitrogen fixation leading to a local increase in biomass. This increase in biomass would increase any pathway sensitivity of atmospheric CO_2. Several studies considering a dynamic land component and focusing on phytoplankton light absorption report an increase in heat budget (**??**). If a land model were to be included, we speculate that we would still find an oceanic and atmospheric heating. However, the magnitude of changes might be smaller due to the uptake of CO_2 by vegetation, decreasing the atmospheric CO_2 concentration. Furthermore, the model does not include a temperature-dependency of iron bioavailability. According to previous experiments, a warming of the ocean decreases the bioavailability of iron (**?**). Phytoplankton light absorption increasing oceanic temperature might thus reduces the iron bioavailability. As a consequence, the limitation of phytoplankton growth by iron would increase, limiting the increase in chlorophyll biomass due to phytoplankton light absorption. Our study only considers two PFTs and bringing in more PFTs would be an interesting complement of our findings. For instance, observations and modeling studies indicate that positively buoyant phytoplankton groups, such as cyanobacteria, are important to study phytoplankton light absorption (**???**). Implementing these microorganisms to assess our research question could be a beneficial follow-up of our study.

6 Conclusions

For the first time, we compare the role of ~~these individual~~ the air-sea heat and CO_2 fluxes and quantify their influence on the biologically-induced atmospheric warming. We show that without any seasonality and with all the climate pathways included, the surface atmospheric temperature increases by 0.14°C due to phytoplankton light absorption. As suggested by **???**previous studies (**???**), phytoplankton light absorption changes the air-sea heat flux. Our results indicate that when only this air-sea interaction is considered, the atmosphere cools by 0.02°C compared to a simulation without the biogeophysical mechanism. Moreover, when only the air-sea CO_2 exchange is considered, the atmospheric temperature increases by 0.71°C. Clearly, our results indicate that the air-sea CO_2 exchange has a more important effect than the air-sea heat flux on the phytoplankton-induced warming of the atmosphere. With our model setup, the sea-ice extent and thickness slightly vary between simulations, therefore sea-ice processes hardly affect the air-sea CO_2 flux and thus the climate system. Moreover, including the solubility pathway changes the heat fluxes, specifically reducing the sensible heat flux and the net longwave heat flux compared to the reference simulation. As a consequence, this climate pathway has a negative effect on the atmospheric temperature. To

conclude, phytoplankton light absorption influences the climate pathways at the ocean-atmosphere interface, particularly the air-sea CO_2 exchange that is important for the phytoplankton-induced atmospheric warming. For future ~~work,~~ climate studies, this work evidences that to capture the overall effect of climate-relevant mechanisms such as phytoplankton light absorption, the atmospheric CO_2 concentrations should evolve freely.

For future work, more studies with higher complexity models are necessary to make quantitative assessments rather than qualitative assessments as in our study. ~~For instance~~Similar simulations must be conducted with a seasonal variation of the shortwave radiation to better understand the role of phytoplankton in the climate system. Moreover, a model with a dynamic atmosphere such as PLASIM-GENIE (**?**) could be a good aspiration to complete our study. ~~Observations and modeling studies indicate that positively buoyant phytoplankton groups, such as cyanobacteria, are important to study the climate system (???). Implementing these microorganisms to assess our research question could be a beneficial follow-up of~~ Indeed, previous studies evidence either an increased wind speed in subpolar regions (**?**) or an enhanced atmospheric dynamics (**??**) due to phytoplankton light absorption. The increased wind speed with a dynamic atmospheric component could thus increase the air-sea CO_2 flux, reinforcing the importance of the CO_2-pathway in our study. ~~Moreover, similar simulations must be conducted with a seasonal variation of the shortwave radiation to better understand the role of phytoplankton in the climate system~~Finally, implementing the new temperature-dependent remineralization scheme (**??**) would affect the biological pump and would be an extension to our findings.

Code availability. The code for the model is hosted on GitHub and can be obtained by cloning or downloading: https://zenodo.org/record/4733736. The configuration file is named "RA.ECO.ra32lv.FeTDTL.36x36x32" and can be found in the directory "EcoGENIE_LA/genie-main/configs". The user-configuration files to run the experiments can be found in the directory "EcoGENIE_LA/genie-userconfigs/RA/Asselotetal_BG". Details of the code installation and basic model configuration can be found on a PDF file (https://www.seao2.info/cgenie/docs/muffin.pdf). Finally, section 9 of the manual provides tutorials on the ECOGEM ecosystem model.

Data availability. TEXT

Code and data availability. TEXT

Sample availability. TEXT

Video supplement. TEXT

Appendix A: Plankton functional types

We base our ecosystem community on the community described by **?**. However, instead of using ~~16~~ 2 plankton functional types (PFTs) with 8 different size classes, we only use 2 PFTs ~~: one phytoplankton group and one zooplankton group~~ with one size class (Appendix A1). We show that the complexity of the ecosystem does not have an important impact on the climate system compared to the effect of phytoplankton light absorption (**?**). Therefore we reduced the ecosystem complexity to increase the computational time of the model.

Appendix B: Multiple size classes

We conduct two additional simulations with a higher ecosystem complexity. These simulations have 6 phytoplankton and 6 zooplankton size-classes as in **?**. The simulation BioLA6 considers phytoplankton light absorption while the simulation Bio6 does not consider it. The results show that the effect of phytoplankton light absorption is reduced with a higher ecosystem complexity compared to the effect of phytoplankton light absorption with a simple ecosystem community. This is due to the higher amount of carbon stored in the living biomass with increasing number of species, thus reducing the effect of phytoplankton light absorption on the atmospheric CO_2 concentration and on the climate system.

Appendix C: Climate sensitivity

To analyze the climate sensitivity of the model, we perform two sensitivity analyses (Appendix C1). Both simulations have the same model setup, restart from the spin-up described previously but their atmospheric CO_2 concentrations differs. The first simulation (Sensi280) has an atmospheric CO_2 concentration of 280 ppm while the second one (Sensi320) has an atmospheric CO_2 concentration of 320 ppm. Furthermore, the simulations Sensi280 and Sensi320 consider phytoplankton light absorption. An increase of 40 ppm in atmospheric CO_2 concentration slightly reduces the chlorophyll concentration but these changes are negligible. The oceanic and atmospheric heat budgets are affected by the changes in atmospheric CO_2 concentration. Increasing the greenhouse gas concentrations increases in turn the SAT and therefore the SST due to the exchange of heat between the ocean and the atmosphere.

Appendix D: Air-sea fluxes interactions

To estimate the unique effect of each climate pathway we ensure that the heat and CO_2 interaction is negligible by conducting sensitivity analyses. Due to the model setup, the flux of CO_2 across the air-sea interface (F_{CO_2}; Eq. 4) depends on the SST via the Schmidt number (**??**). We conduct two comparable sensitivity analyses and study the changes in F_{CO_2}. First, we artificially increase the SST by 1°C (Appendix D1). This increase in SST only enhances F_{CO_2} by $4.26 \cdot 10^{-5}$ mol/m^2/yr, representing a raise of 2.58% of the total air-sea CO_2 exchange. Second, the mean wind speed affects the F_{CO_2} via the gas transfer velocity (k; Eq. 4). We increase the wind speed by 0.2 m/s, which is a comparable forcing of the artificial increase of 1°C of SST.

Indeed, **?** indicates that a SST increase of 1°C would increase the intensity of the atmosphere dynamics and the tropical wind speed by 0.2 m/s. This increase in mean wind speed enhances the F_{CO_2} by $1.44{\cdot}10^{-4}$ mol/m^2/yr, representing an increase of 8.69% of the total air-sea CO_2 flux. Clearly, the changes in wind speed are much larger than the changes in SST hence we consider that the effect of SST on the air-sea CO_2 exchange is small enough to be neglected.

Between our simulations, the maximum change of F_{CO_2} is only 0.21% which, for instance, increases the atmospheric CO_2 concentration by 0.55% and decreases the DOC by 0.71%. This small increase slightly affects the carbon reservoirs in our simulations.

Appendix E: Seasonal and non-seasonal cycle

We compare two model simulations with phytoplankton light absorption. The model setups are similar except that we switched off the seasonal cycle in one simulation. Turning off the seasonal cycle decreases the mean annual SST by 0.77°C. Furthermore, the difference of atmospheric CO_2 concentration is 6 ppm. This difference is due to different SST and therefore different CO_2 solubility between these simulations. ~~These results indicate that switching off the seasonal cycle damps the response of the climate system to phytoplankton light absorption.~~ Our results without seasonality indicate that the difference of SST between BioLA and Bio is 0.14°C. Similar simulations have been conducted with a seasonal cycle and the SST difference is 0.33°C (**?**). The absence of a seasonal cycle reduces the difference of SST between the simulations with and without phytoplankton light absorption.

Appendix F: Sea-ice

The global sea-ice cover and the global sea-ice area between the simulations HCorg and HCorgSI are identical, explaining their identical climate state. Moreover, the variation of sea-ice between all simulations is small. The maximum global sea-ice cover change of 1.42% occurs between the simulations CARB and HCorgSol.

Appendix G: Precipitation

Slight fluctuations in precipitation are visible in the Appendix G1. First of all, the precipitation between *BioLA* and *HCorgSol* are similar and the same is true for the precipitation between *HCorg* and *HCorgSI*. The precipitation rate is the highest in the simulation *BioLA* due to the important specific humidity. In contrast, *HEAT* has a low specific humidity explaining the lowest precipitation rate for this simulation.

Author contributions. All authors designed and developed the concept of the study. RA performed the analysis of the model outputs with inputs from IH. RA drafted the initial version of the manuscript in collaboration with IH. All co-authors read and reviewed the final version of the manuscript.

Competing interests. The authors declare that they have no conflict of interest.

Disclaimer. TEXT

Acknowledgements. Our special thanks go to Félix Pellerin, Maike Scheffold and Laurin Steidle for their valuable comments on the early version of this manuscript. We thank David A. McKay, Alexandre Pohl and an anonymous reviewer for their helpful comments. This work was supported by the Center for Earth System Research and Sustainability (CEN), University of Hamburg, and contributes to the Cluster of Excellence "CLICCS - Climate, Climatic Change, and Society".

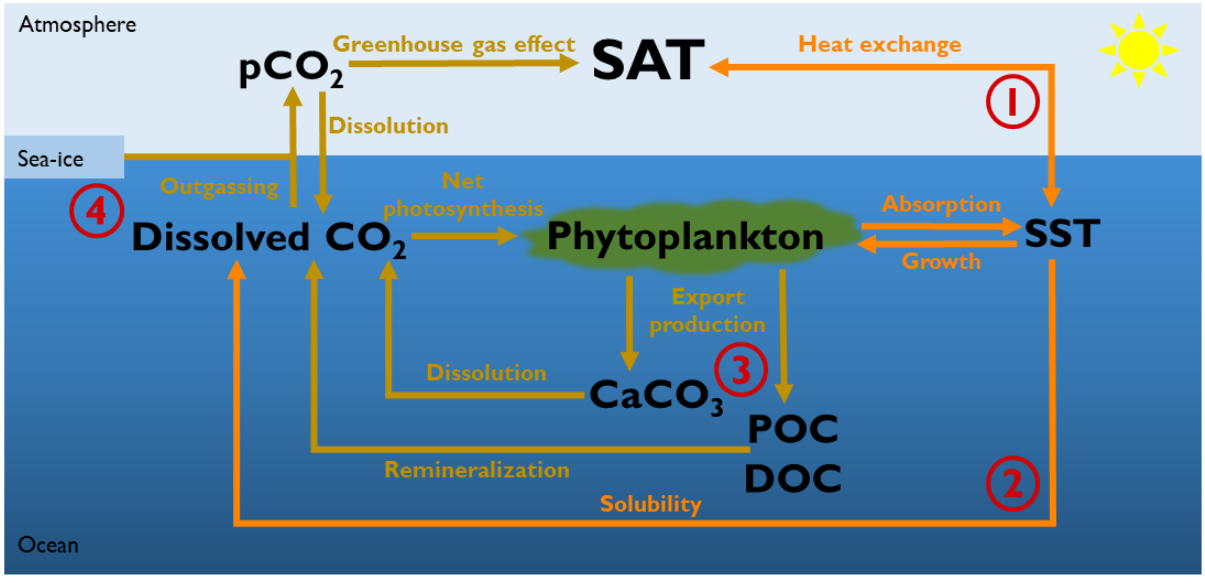

Figure 1. Representation of the four different biologically-induced pathways that affect the atmospheric temperature. (1) Marine biota via phytoplankton light absorption increases the SST, changing therefore the air-sea heat exchange and the atmospheric temperature. (2) Changes in SST also alter the solubility of CO_2 and its dissolved concentration. In turn, changes in dissolved CO_2 concentrations alter the air-sea CO_2 exchange and thus the greenhouse gas effect. (3) Phytoplankton light absorption modifies the marine biogeochemical cycles and particularly the export production of carbon. These changes in export production of carbon modify the dissolved CO_2 concentration and the greenhouse gas effect. (4) A warmer surface of the ocean can decrease the sea-ice extent. A reduction of sea-ice cover increases the air-sea CO_2 exchange area, changing the greenhouse gas concentrations. SAT = surface atmospheric temperature. SST = sea surface temperature. $CaCO_3$ = calcium carbonate. POC = particulate organic carbon. DOC = dissolved organic carbon.

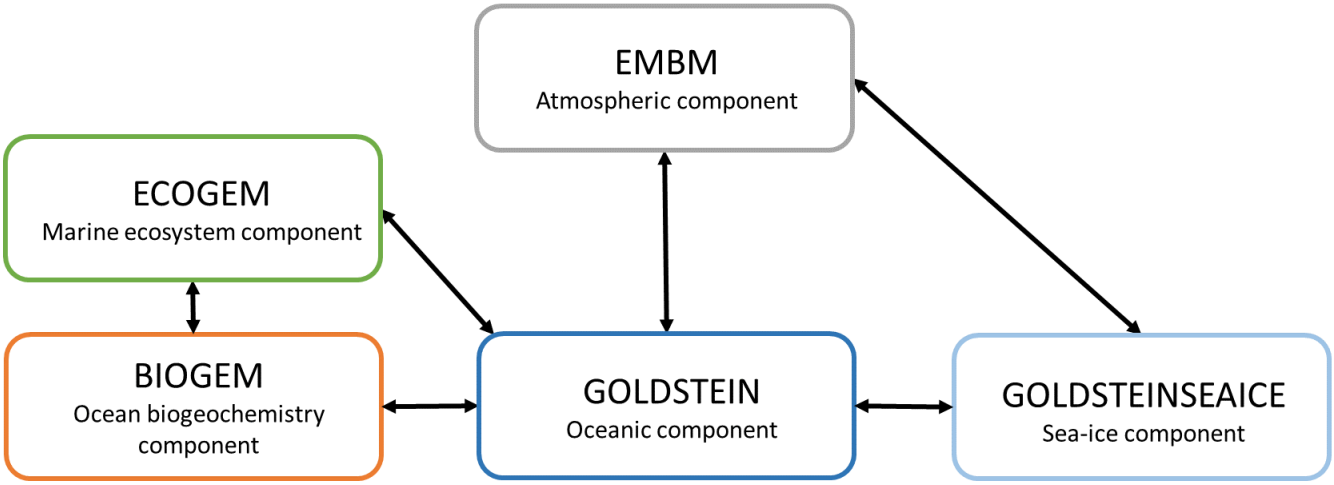

Figure 2. Representation of the components of the ~~EcoGENIE~~ EcoGEnIE model. The black arrows indicate the link between the different climatic components.

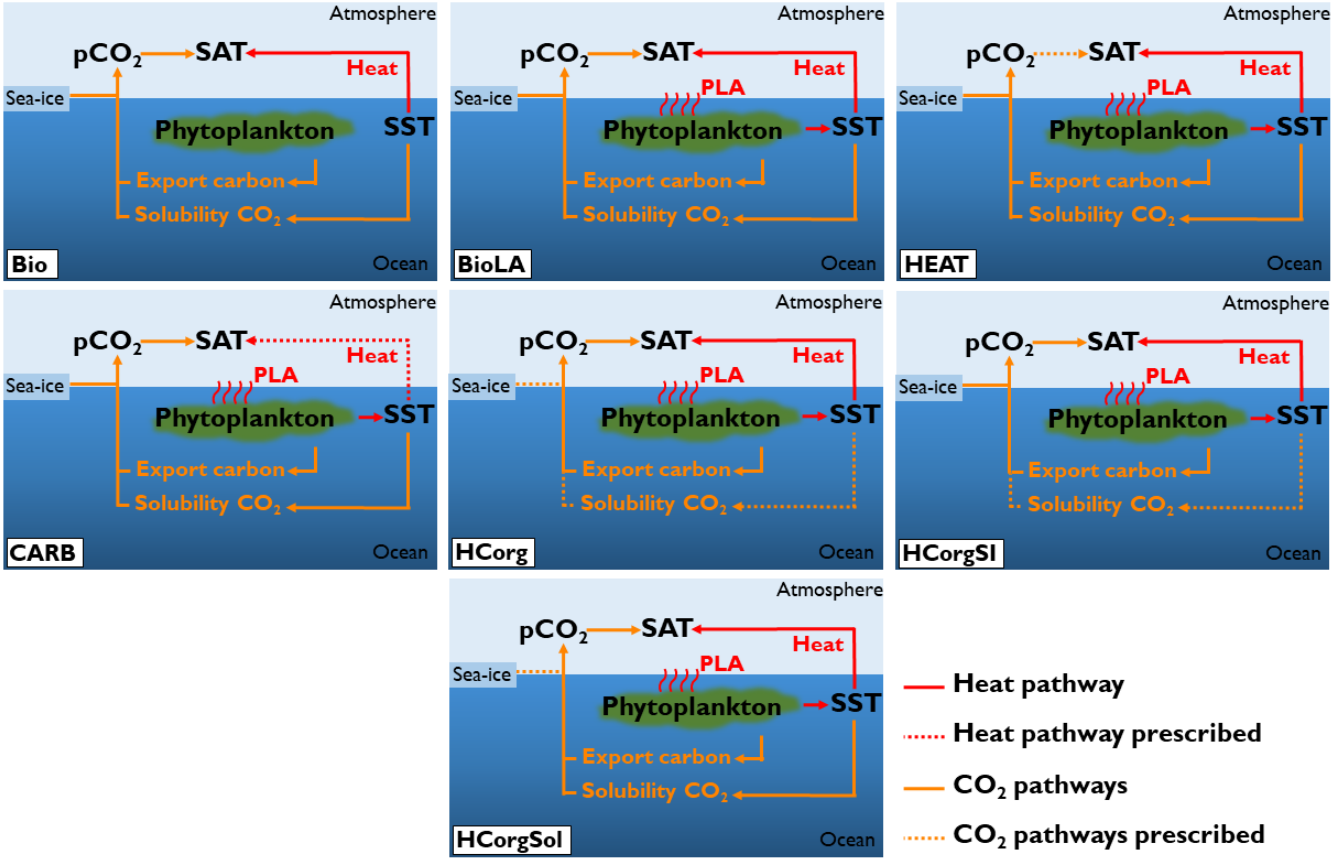

Figure 3. Sketch representing the climate pathways involved in the seven simulations ~~conducted with EcoGENIE~~ (PLA = Phytoplankton Light Absorption). Note that this figure is a simplification of Figure 1, only the relevant pathways are represented. The ~~names~~ name of the simulations are on the bottom left of each panel. The dashed arrows indicate the climate pathways prescribed. All the prescribed pathways are from the reference simulation *Bio* except the pathway between atmospheric CO_2 and SAT in *CARB* which is prescribed from the simulation *BioLA*.

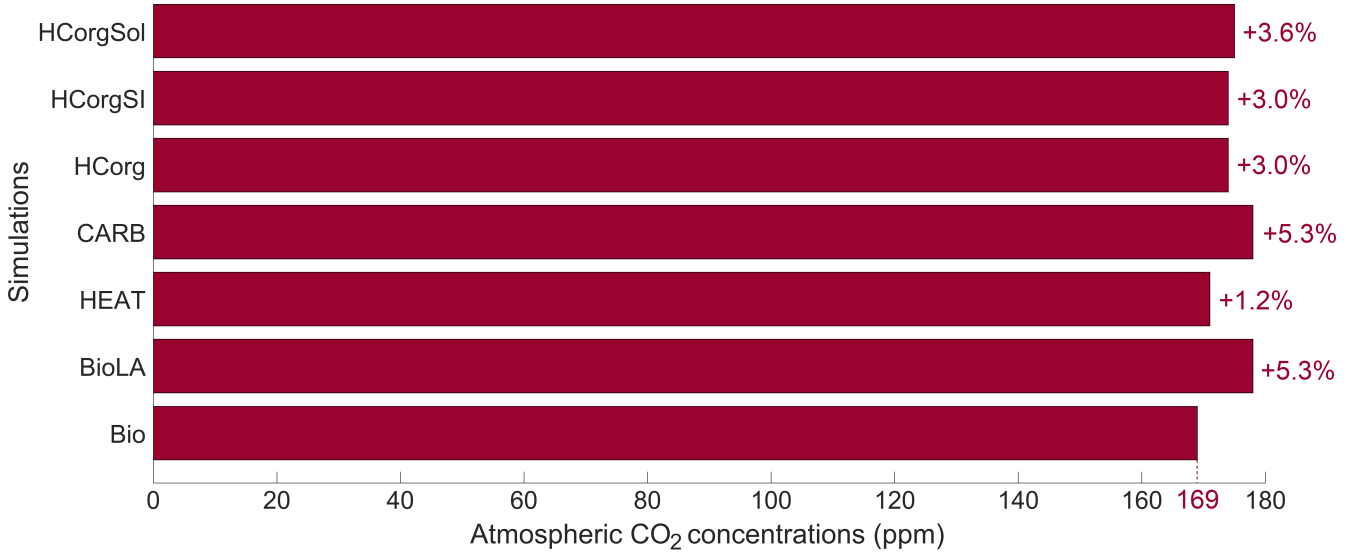

Figure 4. Atmospheric CO_2 concentrations (ppm) for the different simulations. The percentages represent the relative changes compared to the reference simulation Bio.

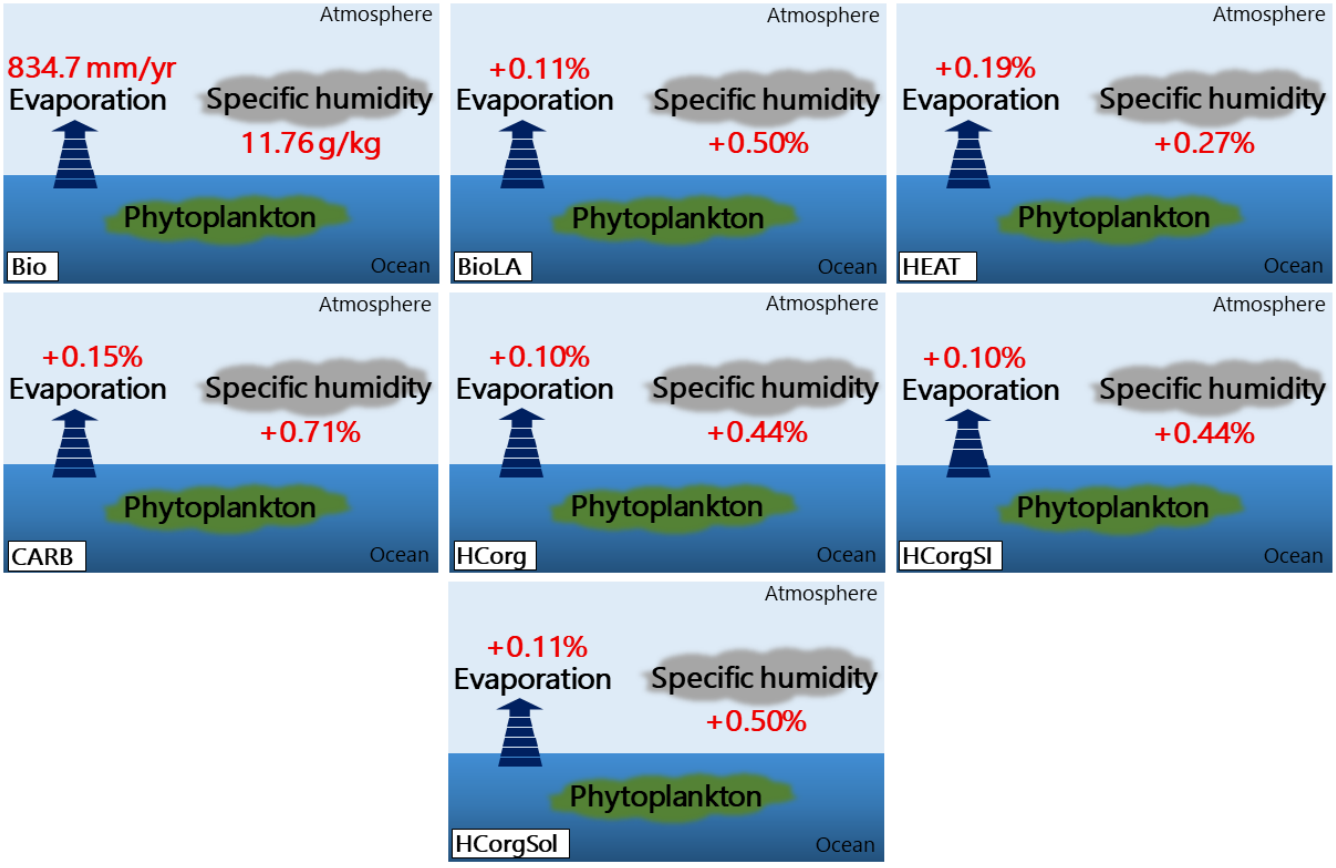

Figure 6. Evaporation (mm/yr) and specific humidity (g/kg) for the seven simulations. The percentages represent the relative changes compared to *Bio*. The name of the simulations are on the bottom left of each panel.

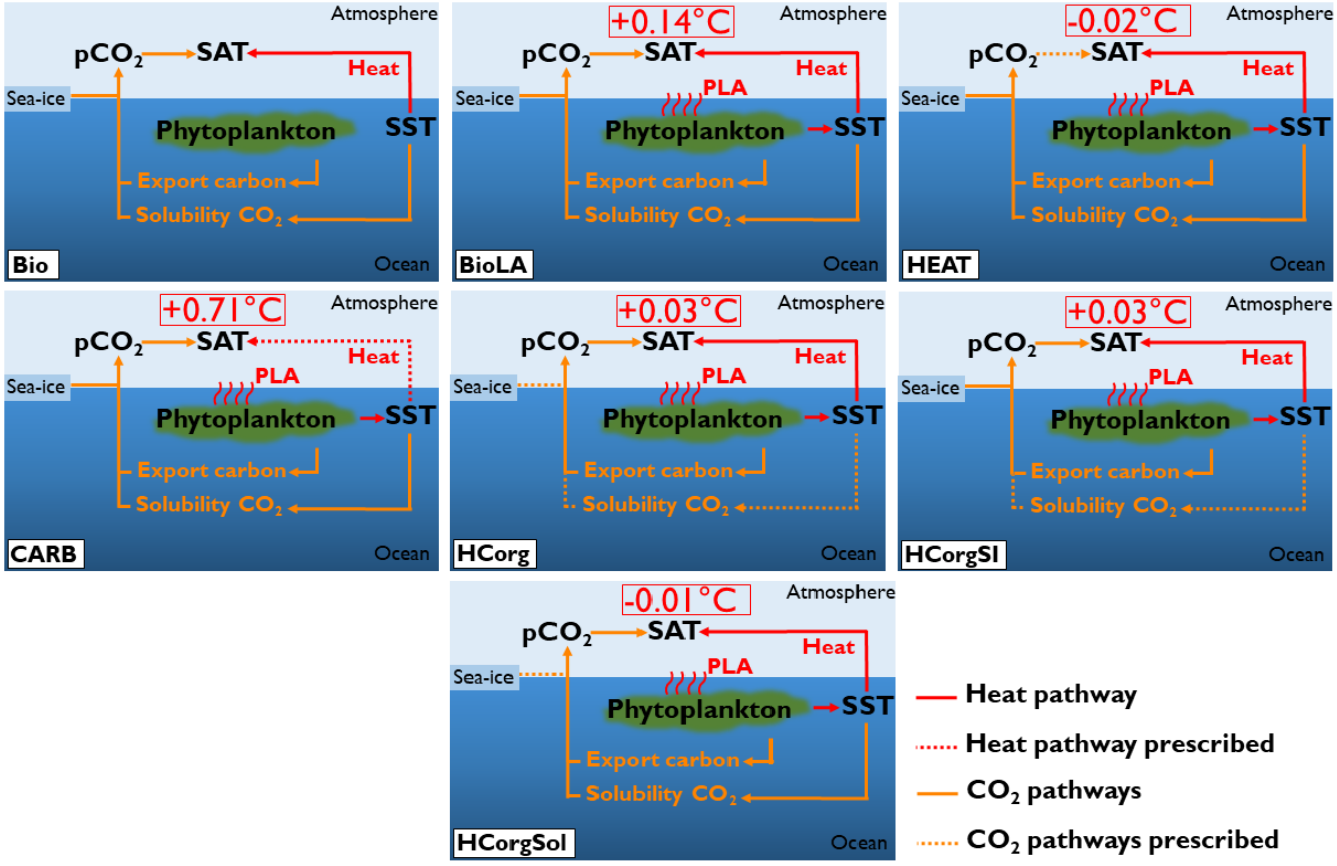

Figure 7. Sketch representing the surface atmospheric temperature (SAT) changes between the simulations and the reference run. On top is located the value of SAT change compared to *Bio*. The rest of the sketch is similar to Figure 3.

Table 1. Sea surface temperature (°C) and surface chlorophyll biomass (mgChl/m^3). There is no value for the simulation CARB because we run the model with an uncoupled ocean-atmosphere setup.

Simulation	SST (°C)	Chlorophyll biomass (mgChl/m^3)
Bio	15.26	0.09949
BioLA	15.34	0.11178
HEAT	15.25	0.10827
CARB	-	-
HCorg	15.30	0.10964
HCorgSI	15.30	0.10964
HCorgSol	15.28	0.10891

Table A1. ~~Comparison~~ Size of the different plankton functional types (~~ppm~~μm) ~~for~~ used during the ~~seven~~ simulations.

PFT	Size (μm)
Phytoplankton	46.25
Zooplankton	146.15

Table B1. ~~Comparison~~ Values of the most important climate quantities for the ~~seven~~ simulations with 6 phyto- and 6 zooplankton size-classes. The third row represents the differences between the simulation with minus without phytoplankton light absorption.

Simulation	Atm. CO_2 (ppm)	Chl. (mgChl/ m^3)	SST (°C)	SAT (°C)
Bio6	154	0.133	14.99	8.93
BioLA6	159	0.140	15.04	8.97
Difference	+5	+0.007	+0.05	+0.04

Table C1. Chlorophyll concentration (mgChl/m^3), sea and atmospheric surface temperature (°C) for the sensitivity analysis of the climate. ~~In~~ The difference represents the value of Sensi320 minus the value of Sensi280.

Simulation	Chloro. conc. (mgChl/m^3)	SST (°C)	SAT (°C)
Sensi280	0.1177	16.78	11.92
Sensi320	0.1175	17.17	12.44
Difference	-0.0002	0.39	0.52

Table D1. Changes in air-sea CO_2 exchange (mol/m^2/yr and %) regarding the sensitivity of the system towards the interplay between CO_2 and heat. For the first sensitivity analysis, the SST is increased by 1°C while for the second analysis, the annual mean wind speed is raised by 0.2 m/s. The third row corresponds to the maximum difference of SST between the simulations.

Sensitivity analysis	F_{CO_2} (mol/m^2/yr)	Changes (%)
+1°C	$+4.26 \cdot 10^{-5}$	2.58
+0.2 m/s	$+1.44 \cdot 10^{-4}$	8.69
+0.08°C	$+3.40 \cdot 10^{-6}$	0.21

Table E1. Sea surface temperature (°C) and atmospheric CO_2 concentration (ppm) for simulations with and without a seasonal cycle.

Simulation	SST (°C)	Atm. CO_2 conc. (ppm)
Seasonal cycle	16.11	184
Non-seasonal cycle	15.34	178

Table F1. Global sea-ice cover (%) and global sea-ice area (km^2) for the different simulations.

Simulation	Sea-ice cover (%)	Sea-ice area (km^2)
Bio	9.79	$3.60 \cdot 10^7$
BioLA	9.76	$3.59 \cdot 10^7$
HEAT	9.91	$3.64 \cdot 10^7$
CARB	8.60	$3.16 \cdot 10^7$
HCorg	~~9.92~~ 9.79	~~3.65~~3.60$\cdot 10^7$
HCorgSI	9.92	$3.65 \cdot 10^7$
HCorgSol	10.02	$3.68 \cdot 10^7$

Table G1. Precipitation (mm/yr) for the different simulations.

Simulation	Precipitation (mm/yr)
Bio	834.62
BioLA	837.07
HEAT	836.30
CARB	834.05
HCorg	837.00
HCorgSI	837.00
HCorgSol	837.07